

Electronic Supplementary Information (ESI) for Chemical Science

This journal is © The Royal Society of Chemistry 2012

Ytterbium(III) porphyrin complex induces endoplasmic reticulum stress and apoptosis in cancer cells: cytotoxicity and transcriptomics studies

Wai-Lun Kwong, Raymond Wai-Yin Sun, Chun-Nam Lok, Fung-Ming Siu, Suk-Yu Wong, Kam-Hung Low and Chi-Ming Che*

Materials and Methods

Materials

Analytical grade organic solvents were used in all experiments unless otherwise stated. Anhydrous ytterbium(III) chloride was purchased from Strem Chemicals Inc. 2,3,7,8,12,13,17,18-Octaethylporphyrin was purchased from Frontier Scientific Inc. *meso*-Tetraphenylporphyrin and its derivatives were synthesized according to procedures described previously. (A. D. Adler, F. R. Longo, J. D. Finarelli, J. Goldmacher, J. Assour and L. Korsakoff, *J. Org. Chem.*, 1967, **32**, 476.) Other chemicals unless otherwise stated were purchased from Sigma-Aldrich Co.

Synthesis and characterization of the ytterbium porphyrin complexes

Ytterbium(III) porphyrin complexes were prepared according to the method of Srivastava with some modifications. (T. S. Srivastava, *Bioinorg. Chem.*, 1978, **8**, 61.) Briefly, a mixture of anhydrous ytterbium(III) chloride (1.9 mmol) and porphyrin ligand (0.19 mmol) was heated in the imidazole melt (3 g) under inert atmosphere for 3 h. After heating, the mixture was cooled to room temperature and the residue was dissolved in a CH₂Cl₂/MeOH solution (9:1, v/v, 20 mL). The solution was filtered and washed with water three times. The organic layer was extracted and dried with anhydrous sodium sulphate. The solution was filtered and the solvent was removed under reduced pressure. The residues were dissolved in minimum amount of CH₂Cl₂ and loaded onto the magnesium carbonate column. Metal-free porphyrin ligand was eluted with CH₂Cl₂/hexane (2:1) and the ytterbium(III) porphyrin product was eluted with CH₂Cl₂/MeOH (25:1). Ytterbium(III) porphyrin complexes were obtained by recrystallization in CH₂Cl₂/EtOH at room temperature.

Ytterbium(III) octaethylporphyrin (OEP) [Yb(OEP)(μ -OH)]₂ (1) Yield = 123 mg, (0.08 mmol, 88%). UV-vis (CH₂Cl₂) λ_{max} / nm (log ϵ): 405 (5.59), 536 (4.42), 572 (4.55). MS-ESI (+ve): 1446 ([Yb(OEP)(μ -OH)]₂+H)⁺. anal. Calcd for C₇₂H₉₀N₈O₂Yb₂·2H₂O (%): C, 58.14; H, 6.61; N, 7.38 Found: C, 58.34; H, 6.39; N, 7.56.

Ytterbium(III) 5,10,15,20-tetraphenylporphyrin (TPP) [Yb(TPP)(μ -OH)]₂ (2) Yield = 118 mg (0.07 mmol, 76%). UV-vis (CH₂Cl₂) λ_{max} / nm (log ϵ): 424 (5.62), 555

(4.26), 592 (3.69). MS-ESI (+ve): 1608 ($[\text{Yb}(\text{TPP})(\mu\text{-OH})]_2 + \text{H}^+$), 1678 ($[\text{Yb}(\text{TPP})(\mu\text{-OH})]_2 + 2 \text{H}_2\text{O} + 2 \text{MeOH}^+$). anal. Calcd for $\text{C}_{88}\text{H}_{58}\text{N}_8\text{O}_2\text{Yb}_2 \cdot 2\text{H}_2\text{O}$ (%): C, 64.67; H, 4.05; N, 6.82 Found: C, 64.39; H, 3.81, N; 6.83.

Ytterbium(III) 5,10,15,20-tetrakis(p-tolyl)porphyrin (TTP) $[\text{Yb}(\text{TPP})(\mu\text{-OH})]_2$ (3)
Yield = 115 mg (0.06 mmol, 66%). UV-vis (CH_2Cl_2) $\lambda_{\text{max}} / \text{nm}$ (log ϵ): 424(5.70), 554 (4.34), 593 (3.94) MS-ESI(+ve): 873.9 ($\text{YbTTP} + \text{MeOH}^+$), 1717 ($[\text{Yb}(\text{TPP})(\mu\text{-OH})]_2 + \text{H}^+$). Calcd. for $\text{C}_{96}\text{H}_{74}\text{N}_8\text{O}_2\text{Yb}_2 \cdot \text{CH}_2\text{Cl}_2 \cdot 2\text{H}_2\text{O}$ (%): C, 63.36; H, 4.39; N, 6.09 Found: C, 63.04; H, 4.59; N, 6.17.

Ytterbium(III) 5,10,15,20-tetrakis(p-chlorophenyl)porphyrin (TCP) $[\text{Yb}(\text{TCP})(\mu\text{-OH})]_2$ (4) Yield = 94 mg (0.05 mmol, 48%). UV-vis (CH_2Cl_2) $\lambda_{\text{max}} / \text{nm}$ (log ϵ): 424 (5.65), 554 (4.31), 593 (3.79) MS-ESI (+ve): 1004 ($\text{YbTCP} + 2 \text{MeOH} + \text{H}_2\text{O}^+$), 1981 ($[\text{Yb}(\text{TCP})(\mu\text{-OH})]_2 + 2 \text{H}_2\text{O} + 2 \text{MeOH}^+$). Calcd. for $\text{C}_{88}\text{H}_{50}\text{Cl}_8\text{N}_8\text{O}_2\text{Yb}_2 \cdot 2\text{CH}_2\text{Cl}_2 \cdot \text{H}_2\text{O}$ (%): C, 52.25; H, 2.73; N, 5.42 Found: C, 52.01; H, 2.87; N, 5.41.

X-ray crystallography

Crystals of **1** were obtained from recrystallization ($\text{CH}_2\text{Cl}_2/\text{EtOH}$ or DMSO) at room temperature. For the crystal obtained in $\text{CH}_2\text{Cl}_2/\text{EtOH}$, red crystal with dimensions $0.30 \times 0.20 \times 0.05$ mm mounted in a glass capillary was used for data collection at 253 K on a MAR diffractometer with a 300 mm image plate detector using graphite monochromatized Mo- K_α radiation ($\lambda = 0.71073 \text{ \AA}$). The crystal structure was solved by direct methods employing SHELXS-97 program. (G. M. Sheldrick, *Acta. Cryst.*, 2008, **A64**, 112) Yb and other non-H atoms were located according to the direct methods. The positions of the other non-hydrogen atoms were found after successful refinement by full-matrix least-squares using program SHELXL-97. Bridging O atoms were disordered by rotation of the molecule and it is a double $-\mu\text{-O}$ bridging compound. One water O was also disordered which may concern the disorderness of the O-bridging. Another water O was also located.

Recrystallization of **1** in DMSO under ambient conditions provided another type of crystals. A crystal with dimensions $0.08 \times 0.06 \times 0.04$ mm mounted in a glass

capillary was used for data collection at 296 K on a Bruker X8 Proteum diffractometer using MICROSTAR rotating anode Cu-K_α radiation ($\lambda = 1.54178 \text{ \AA}$) and a Pt135 CCD detector. The structure was solved by direct methods employing SHELXS-97 program. Yb and non-H atoms were located according to the direct methods and refined by full-matrix least-squares using program SHELXL-97.

Crystal of **2** was obtained from recrystallization (CH₂Cl₂/EtOH) at room temperature. A crystal of dimensions 0.5 × 0.2 × 0.1 mm mounted in a glass capillary was used for data collection at 301 K on a Bruker Smart CCD 1000 using graphite monochromatized Mo-K_α radiation ($\lambda = 0.71073 \text{ \AA}$). The crystal structure was solved by direct methods employing SHELXS-97 program. Yb and other non-H atoms were located according to the direct methods. The positions of the other non-hydrogen atoms were found after successful refinement by full-matrix least-squares using program SHELXL-97.

Cell cultures

All cell lines were obtained from American Type Culture Collection (ATCC). Human cervical epithelial carcinoma (HeLa), human hepatocellular carcinoma (HepG2), human breast carcinoma (MCF-7) and human normal lung fibroblast (CCD-19Lu) were maintained in Eagle's minimum essential medium. Human colorectal carcinoma (SW480) was maintained in Dulbecco's modified Eagle's medium. Human non-small lung cancer (NCI-H460) was maintained in RPMI-1640 medium. All cell culture media were supplemented with 10% v/v fetal bovine serum, L-glutamine (2 mM) and penicillin/streptomycin (100 U/mL). Cells were incubated in 5% CO₂ humidified air atmosphere at 310 K and subcultured when 80% confluence was reached.

Cytotoxicity assay

The cytotoxic properties of the ytterbium porphyrin complexes were evaluated by 3-(4,5-dimethylthiazol-2-yl)-2,5-diphenyltetrazolium bromide (MTT) assay. (T. Mosmann, *J. Immunol. Methods*, 1983, **65**, 55) Briefly, cells were seeded in 96-well plates and incubated for overnight prior to be examined. Powder ytterbium(III) porphyrin complexes were dissolved in DMSO. The concentration of the complexes was calculated according to the elemental composition of the complexes determined

by the elemental analyses. Media in the presence of the tested ytterbium porphyrin complexes were added and serially diluted to various concentrations (from 10 μM to 39 nM), and media containing cisplatin were used as the positive control. The maximum concentration of DMSO in media did not exceed 0.1% (v/v). The cells were incubated for 48 h and followed by the addition of MTT solution. The cells were further incubated for 3 h and sodium dodecylsulfate solution (10% w/v) was subsequently added. The absorption intensities at 580 nm in each well were measured by a Perkin-Elmer FusionTM α -FP plate reader. The IC_{50} values of the complexes (concentrations at which could inhibit cellular growth by 50% compared to the negative control) were determined from the plots of the cell viability percentage *versus* the complex concentration.

Cellular uptake

HeLa cells (2×10^5) treated with **1** (1 μM) or YbCl_3 (2 μM) were incubated for 6, 12 and 24 h. After treatment, cells were washed three times with PBS and MilliQ water (500 μL) was subsequently added. The cells were digested by an equal volume of HNO_3 (70%) for 12 h, and were diluted ten-fold by MilliQ water for ICP-MS analysis. Ytterbium was measured as atomic mass unit (amu) of 173. The cellular ytterbium concentrations were normalized by cellular protein concentration.

Total RNA extraction

Total RNA was isolated using Trizol protocol. HeLa cells were washed with PBS and homogenized in Trizol after **1** (1 μM) treatment for 7 h. Chloroform was added followed by vigorous shaking for 15 s. The aqueous layers were collected after centrifugation (13200 rpm, 5 min). Equal volumes of isopropanol were added and the solutions were incubated at on ice for 2 h to allow complete RNA precipitation. The supernatants were discarded after centrifugation. The remaining portions were washed twice with ethanol (70%), re-dissolved in RNAase-free water and purified by an RNeasy[®] Mini Kit. The purity of the RNA samples was examined by using Agilent RNA 6000 Pico Kit (Agilent, Santa Clara, CA) in Agilent 2100 Bioanalyzer (Agilent).

Microarray and bioinformatics analysis

The gene expression profiles of **1**-treated and untreated samples were compared by Affymetrix Human Genome U133 Plus 2.0 microarray. All of the samples were

assayed in triplate. Hybridization and fluorescence labeling of extracted RNA were performed at Centre for Genome Sciences, Li Ka Shing Faculty of Medicine, The University of Hong Kong. The data analysis was performed by the statistical package BRB-ArrayTools using MAS-normalization. The statistically significant genes were identified by SAM algorithm. A total of 128 probe sets were regulated upon the drug treatment. The gene lists were submitted to connectivity map analysis to identify the drug with similar gene signatures.

Flow cytometry

The percentage of apoptotic and necrotic cells were measured by annexin-V-Alexa Fluor 647/SYTOX[®] green (SG) (Molecular Probes, Invitrogen) double staining flow cytometry. HeLa cells were treated with **1** (1 μ M) for 24 and 48 h and the cells treated with staurosporine (200 nM) was used as a positive control. Cells were trypsinized, collected by centrifugation and re-suspended in 10 mM HEPES buffer (140 mM NaCl and 2.5 mM CaCl₂ at pH 7.4). Cells were incubated with annexin-V conjugated with Alexa Fluor 647 and SG for 20 min at 310 K. Cells were kept on ice until the flow cytometric analysis. The percentage of viable (annexin negative/ SG negative), apoptotic (annexin positive/SG negative) and necrotic cells (annexin positive/SG positive) were measured by Becton Dickson (BD) FACScalibur flow cytometer and analyzed with Cellquest Pro software.

For determination of proteasome inhibition, Ub^{G76V}-YFP transfected HeLa (2×10^5) cells were treated with **1** (1 μ M) for 24 h. After treatment, cells were trypsinized and re-suspended in ice-cooled PBS. Flow cytometry was performed with BD FACScalibur flow cytometer and analyzed with Cellquest Pro software. Treatment of MG-132 proteasome inhibitor (5 μ M) for 24 h was used as a positive control.

Transmission electron microscopy

HeLa cells (1×10^6) were seeded in 10-cm dishes with completed culture medium, After 24 h of incubation, medium containing **1** was used to replace the original one and the cell cultures were incubated for an addition of 7 h at 310 K. The cells were washed twice with PBS, trypsinized, collected, and centrifuged at 1500 rpm for 5 min. The cells were washed twice again with PBS and fixed with 2.5% glutaraldehyde in cacodylate buffer (0.1M sodium cacodylate-HCl pH 7.4) for overnight at 4°C. The

cells were post-fixed with 1% osmium tetroxide in the cacodylate buffer for 1 h at room temperature and dehydrated by treating with increasing concentrations of ethanol (50%, 70%, 90% and 100% 3 times) and finally propylene oxide. The fixed cells were infiltrated with epoxy resin/propylene oxide (1:1) mixture for 90 min at 310 K in a vacuum oven, embedded in fresh epoxy resin and left for polymerization at 333 K for overnight. The resin blocks were cut into ultra-thin sections and stained with 2% aqueous uranyl acetate and lead citrate. Stained sections were observed using a Philips 301 transmission electron microscope at 80 kV for TEM analysis.

Mitochondrial membrane depolarization and mitochondrial swelling

To monitor the change in mitochondrial membrane potential, 5,5',6,6'-tetrachloro-1,1',3,3'-tetraethylbenzimidazolyl carbocyanine iodide (JC-1) (Molecular Probe, Invitrogen) was used. HeLa cells (1×10^5) were treated with **1** (1 μ M) for 7 and 24 h. After the incubation, media were removed and the cells were washed with serum-free medium twice. The cells were stained with JC-1 (5 μ M) in serum free medium for 30 min at 310 K under 5% CO₂ atmosphere. The staining solutions were removed and replaced by serum-free medium. The cells were observed under fluorescence microscope. To examine mitochondria swelling, the cells were stained with MitoTracker® orange (100 nM, Molecular Probes, Invitrogen) with same procedures described above.

Western blotting analysis

HeLa cells (5×10^5) were cultured on 60 mm dish and incubated overnight before experiments. HeLa cells were treated with **1** (1 μ M) for various incubation periods (12, 18, 24 and 30 h). At the end each incubation period, cells were harvested and lysed using the lysis buffer (150 mM NaCl, 100 mM Tris-HCl pH 7.4, 10% glycerol, 1% Triton X-100, 10 mM NaF, 5 mM sodium pyrophosphate, 5 mM sodium orthovanadate, 0.1% SDS) with protease inhibitor cocktail. Total protein extracts (40 μ g) were loaded onto 12.5% SDS-polyacrylamide gel, separated by electrophoresis followed by transfer of proteins from the gel to polyvinylidene fluoride (PVDF) membranes. After the transfer of protein, the membrane was then blocked with 3% BSA in TBST buffer and incubated with corresponding primary antibodies at 4°C overnight. Primary antibodies of anti-cleaved caspase 9 (1:1500), anti-cleaved PARP

(1:1500), anti-CHOP (1:1000), anti-phospho-eIF2 α (1:1000) were obtained from Cell Signaling Technology. After washing, the membrane was incubated with secondary antibody conjugated with horseradish peroxidase (1:5000) for 90 min. The immunoreactive signals were detected using enhanced chemoluminescence kit (GE healthcare) following the procedures given in the user manual. Equal loading of each lane was confirmed by the intensity of β -actin.

Reverse transcriptase-polymerase chain reaction (RT-PCR)

Primers were purchased from Tech Dragon Limited and Genome Research Centre, The University of Hong Kong. Reverse transcription and PCR of extracted RNA were performed using SuperScriptTM III One-Step RT-PCR System with Platinum[®] *Taq* (Invitrogen). The following parameters were used: cDNA synthesis and pre-denaturation (323 K for 30 min followed by 367 K for 2 min), PCR amplification (denatured at 367 K for 20 s, annealed at 328 K for 1 min and extend at 341 K for 1 min) and final extension (345 K for 7 min). The sequences of the primers were shown as follows: *CHOP*: 5'-TCT GGC TTG GCT GAC TGA GGA GG A -3' (forward), 5'-TGG TGC AGA TTC ACC ATT CGG TCA -3' (reverse); *Xbp-1*: 5'-CTGGAACAGCAAGTGGTAGA-3' (forward), 5'-CTG GGT CCT TCT GGG TAG AC-3' (reverse); *ATF3*: 5'- CAG GAT GCC CAC CGT TAG GAT TCA-3' (forward), 5'-TTT GCA ACA GAG GAC CTG CCA TCA -3' (reverse), *ASNS*, 5'-TTG GAA TGC AGC CAA TTC GAC GA -3' (forward), 5'-AAG GGA GTC GCG GAG TGC TTC AAT -3' (reverse); *ChaC*, 5'-AAG TAC CTG AAT GTG CGA GAG GCA -3' (forward), 5'- AGT ATT CAA GGT TGT GGC CGG AGA -3' (reverse) ; *CEBPG*: 5'-AGG CCG CGC AGA AGG TTC TTG -3' (forward), 5'-ACA GCC CCA TGG CAG CTA TTT TGA -3' (reverse); *GAPDH*: 5'-ACC ACA GTC CAT GCC TAC AC -3' (forward), 5'-TTC ACC ACC CTG TTG CTG TA -3' (reverse)

Table S1. Crystal data and structural refinement for **1** and **2**

	1 (recrystallized in CH ₂ Cl ₂ /EtOH)	1 (recrystallized in DMSO)	2 (recrystallized in CH ₂ Cl ₂ /EtOH)
Empirical formula	C ₇₂ H ₉₄ N ₈ O ₄ Yb ₂	C ₈₀ H ₁₁₄ N ₈ O ₈ S ₄ Yb ₂	C ₁₈₀ H ₁₂₂ N ₁₆ O ₉ Yb ₄
Formula weight	1481.63	1790.15	3345.10
Temperature	253 K	296 K	301 K
Wavelength	0.71073 Å	1.54178	0.71073 Å
Crystal system	Monoclinic	Monoclinic	Monoclinic
Space group	P 2 ₁ /n	P 2 ₁ /n	P 2 ₁ /n
Until cell dimensions	a = 21.626(4)Å, α = 90°, b = 15.247(3) Å, β = 115.48(3)°, c = 23.238(5) Å, γ = 90°	a = 11.3252(4)Å, α = 90°, b = 14.7748(5) Å, β = 90.686(2)°, c = 24.3057(5)Å, γ = 90°	a = 15.166(3) Å, α = 90°, b = 19.459(3) Å, β = 103.55(2)°, c = 26.213(4) Å, γ = 90°
Volume	6917(2) Å ³	4066.7(2) Å ³	7521(2) Å ³
Z	4	2	2
Density (calculated)	1.423 g cm ⁻³	1.462 g cm ⁻³	1.477 g cm ⁻³
Absorption coefficient	2.740 mm ⁻¹	5.555 mm ⁻¹	2.530 mm ⁻¹
F(000)	3016	1836	3332
Crystal size	0.3 × 0.2 × 0.05 mm	0.08 × 0.06 × 0.04 mm	0.5 × 0.2 × 0.1 mm
Theta range for data collection	1.08 to 23.78°	3.5 to 65.5°	1.73 to 27.88°
Index ranges	-21 ≤ h ≤ 20, -15 ≤ k ≤ 16, -25 ≤ l ≤ 24	-13 ≤ h ≤ 12, -16 ≤ k ≤ 16, -28 ≤ l ≤ 28	-18 ≤ h ≤ 18, 19, -25 ≤ k ≤ 25, -33 ≤ l ≤ 27
Reflections collected	22824	49197	41255
Independent reflections	6895 [R(int) = 0.0945]	6698 [R(int) = 0.046]	14271 [R(int) = 0.0504]
Refinement method	full-matrix least-squares refinement on F ²	full-matrix least-squares refinement on F ²	full-matrix least-squares refinement on F ²
Data/restraints/parameters	6895/0/407	6698/0/480	14271/0/937
Goodness-of-fit on F ²	0.855	1.074	1.036
Final R indices [I/2 sigma(I)]	R ₁ = 0.0641, wR ₂ = 0.151	R ₁ = 0.0495, wR ₂ = 0.1183	R ₁ = 0.0514, wR ₂ = 0.1762
Largest diff. Peak and hole	1.268 and -1.386 eÅ ⁻³	1.42 and -1.11 eÅ ⁻³	1.285 and -1.599 eÅ ⁻³

Table S2. Selected bond distances (Å) and bond angles (°) for **1** and **2**

1 (recrystallized in CH ₂ Cl ₂ /EtOH)			
Yb(1) – N(1)	2.292	Yb(2) – N(5)	2.311
Yb(1) – N(2)	2.322	Yb(2) – N(6)	2.336
Yb(1) – N(3)	2.316	Yb(2) – N(7)	2.352
Yb(1) – N(4)	2.301	Yb(2) – N(8)	2.337
Yb(1) – O(1)	2.407	Yb(2) – O(1)	2.418
Yb(1) – O(2)	2.241	Yb(2) – O(2)	2.250
N(1) – Yb(1) – N(2)	77.43	N(5) – Yb(2) – N(6)	78.28
N(2) – Yb(1) – N(3)	79.24	N(6) – Yb(2) – N(7)	77.51
N(3) – Yb(1) – N(4)	76.16	N(7) – Yb(2) – N(8)	77.78
N(4) – Yb(1) – N(1)	79.39	N(8) – Yb(2) – N(5)	78.40
O(1) – Yb(1) – O(2)	82.54	O(1) – Yb(2) – O(2)	82.11
1 (recrystallized in DMSO)			
Yb(1) – N(1)	2.343	Yb(1) – N(3)	2.330
Yb(1) – N(2)	2.312	Yb(1) – N(4)	2.333
Yb(1) – O(1)	2.313	Yb(1) – O(2)	2.409
Yb(1) – O(3)	2.327		
N(1) – Yb(1) – N(2)	76.73	N(2) – Yb(2) – N(3)	77.44
N(3) – Yb(1) – N(4)	76.33	N(6) – Yb(2) – N(7)	77.23
O(1) – Yb(1) – O(2)	72.32	O(2) – Yb(1) – O(3)	67.22
O(3) – Yb(1) – O(1)	78.45		

2 (recrystallized in CH ₂ Cl ₂ /EtOH)			
Yb(1) – N(1)	2.324	Yb(2) – N(5)	2.327
Yb(1) – N(2)	2.328	Yb(2) – N(6)	2.300
Yb(1) – N(3)	2.323	Yb(2) – N(7)	2.320
Yb(1) – N(4)	2.326	Yb(2) – N(8)	2.290
Yb(1) – O(1)	2.240	Yb(2) – O(1)	2.178
Yb(1) – O(2)	2.249	Yb(2) – O(2)	2.204
Yb(1) – O(3)	2.464		
<hr/>			
N(1) – Yb(1) – N(2)	76.28	N(5) – Yb(2) – N(6)	77.93
N(2) – Yb(1) – N(3)	76.31	N(6) – Yb(2) – N(7)	78.08
N(3) – Yb(1) – N(4)	77.03	N(7) – Yb(2) – N(8)	78.55
N(4) – Yb(1) – N(1)	76.51	N(8) – Yb(2) – N(5)	78.21
O(1) – Yb(1) – O(2)	70.79	O(1) – Yb(2) – O(2)	72.80

Fig. S1a Perspective view of **1** (recrystallized in $\text{CH}_2\text{Cl}_2/\text{EtOH}$) with 30% probability thermal ellipsoids.

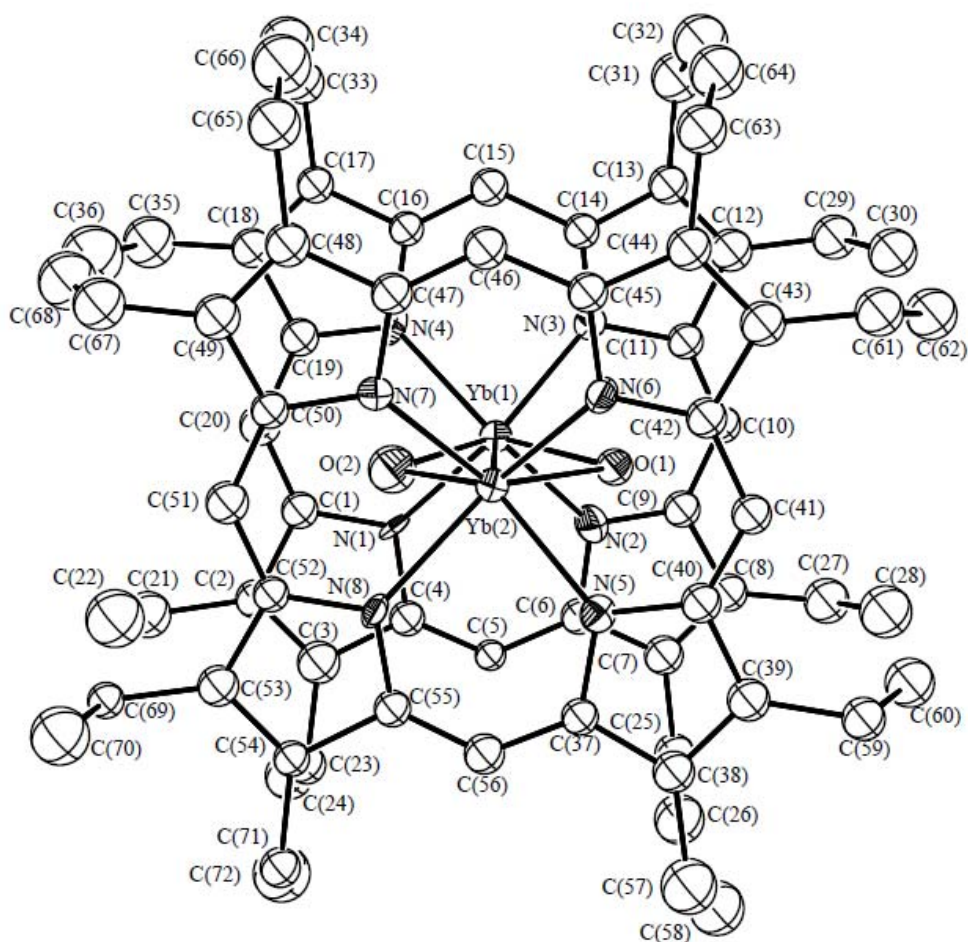


Fig. S1b Perspective view of **2** with 30% probability thermal ellipsoids

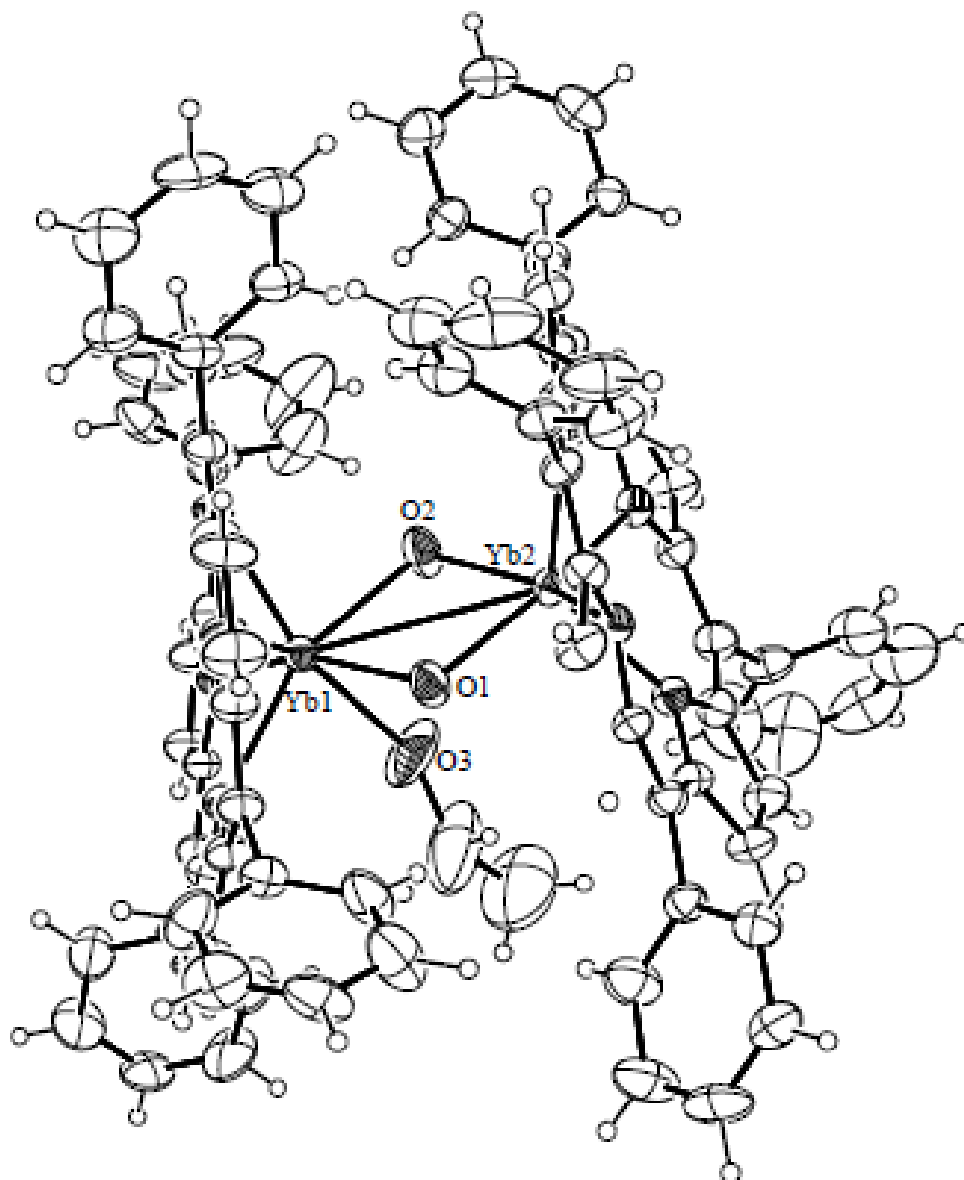


Fig. S2. ESI-MS spectrum of **1** in DMSO/MeOH (1:99)

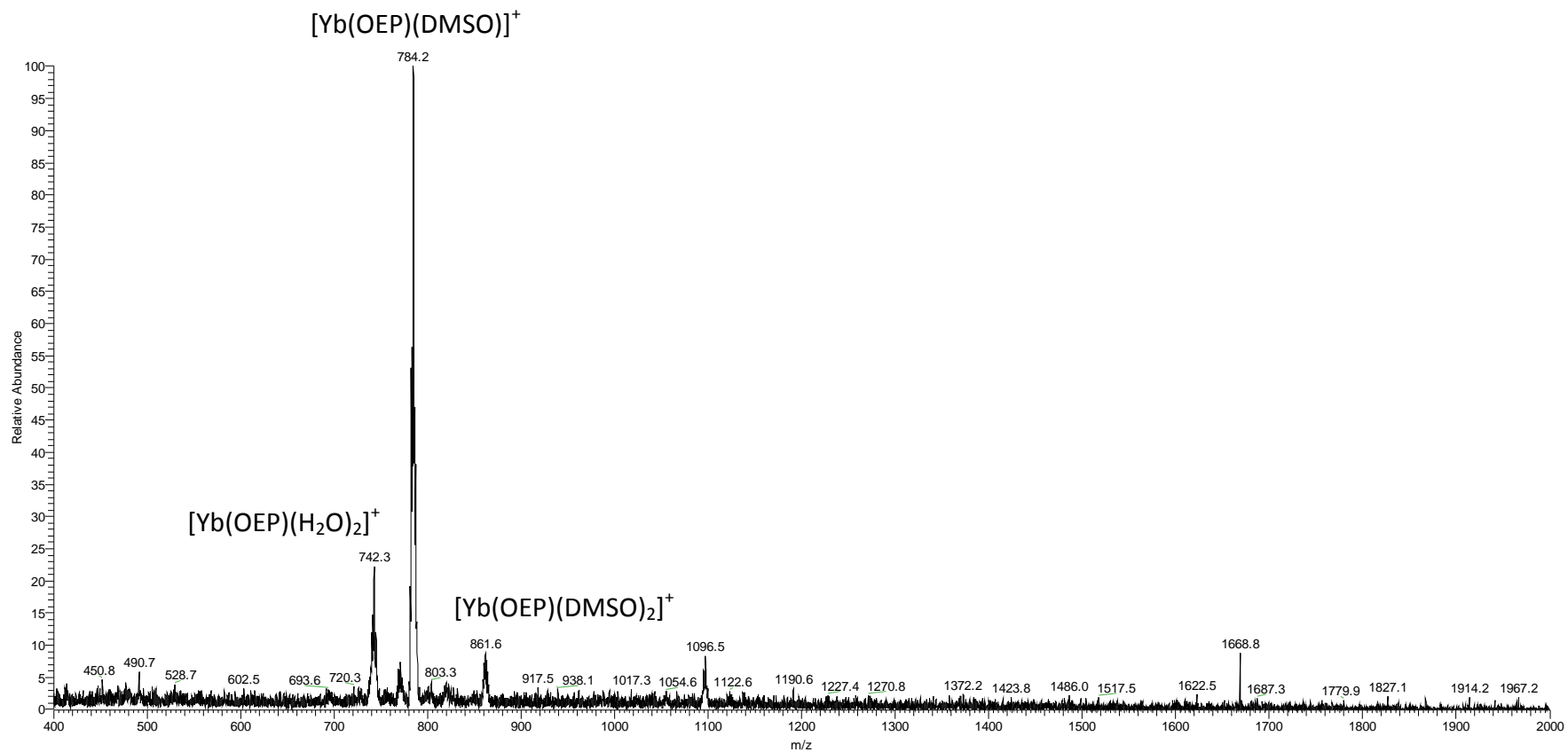


Fig. S3. ESI-MS spectrum of **2** in DMSO/MeOH (1:99)

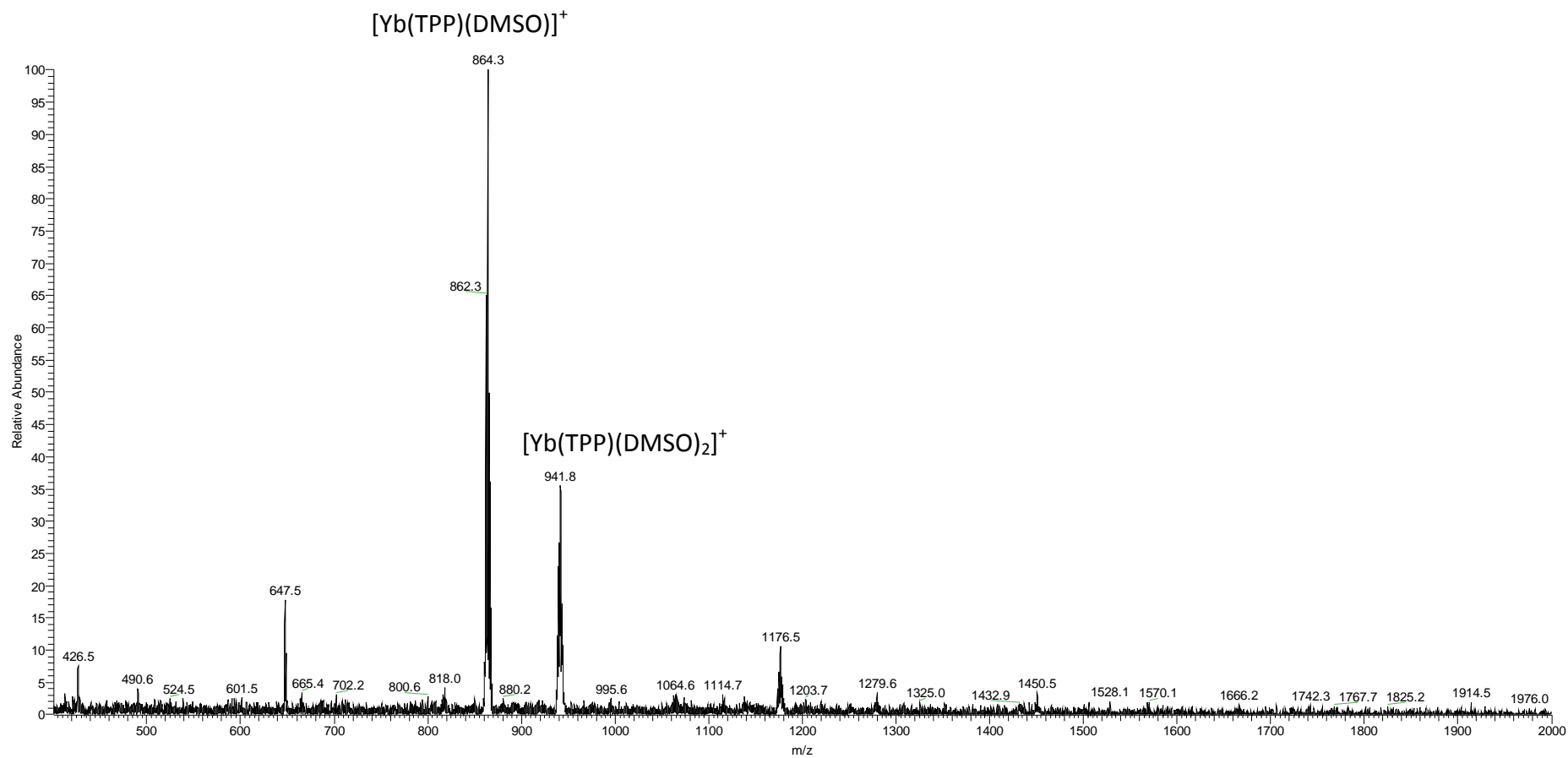


Fig. S4. ESI-MS spectrum of **3** in DMSO/MeOH (1:99)

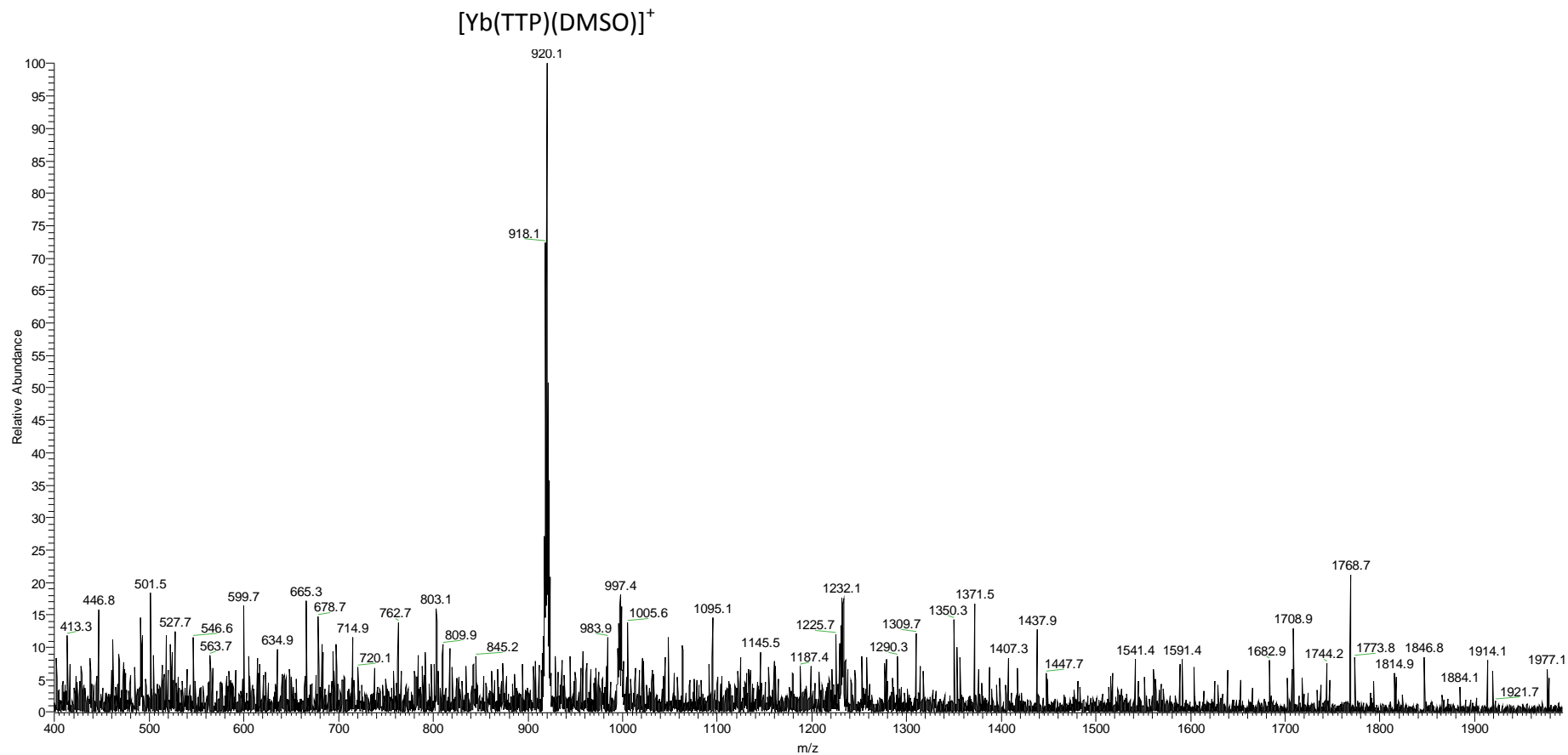


Fig. S5. ESI-MS spectrum of **4** in DMSO/MeOH (1:99)

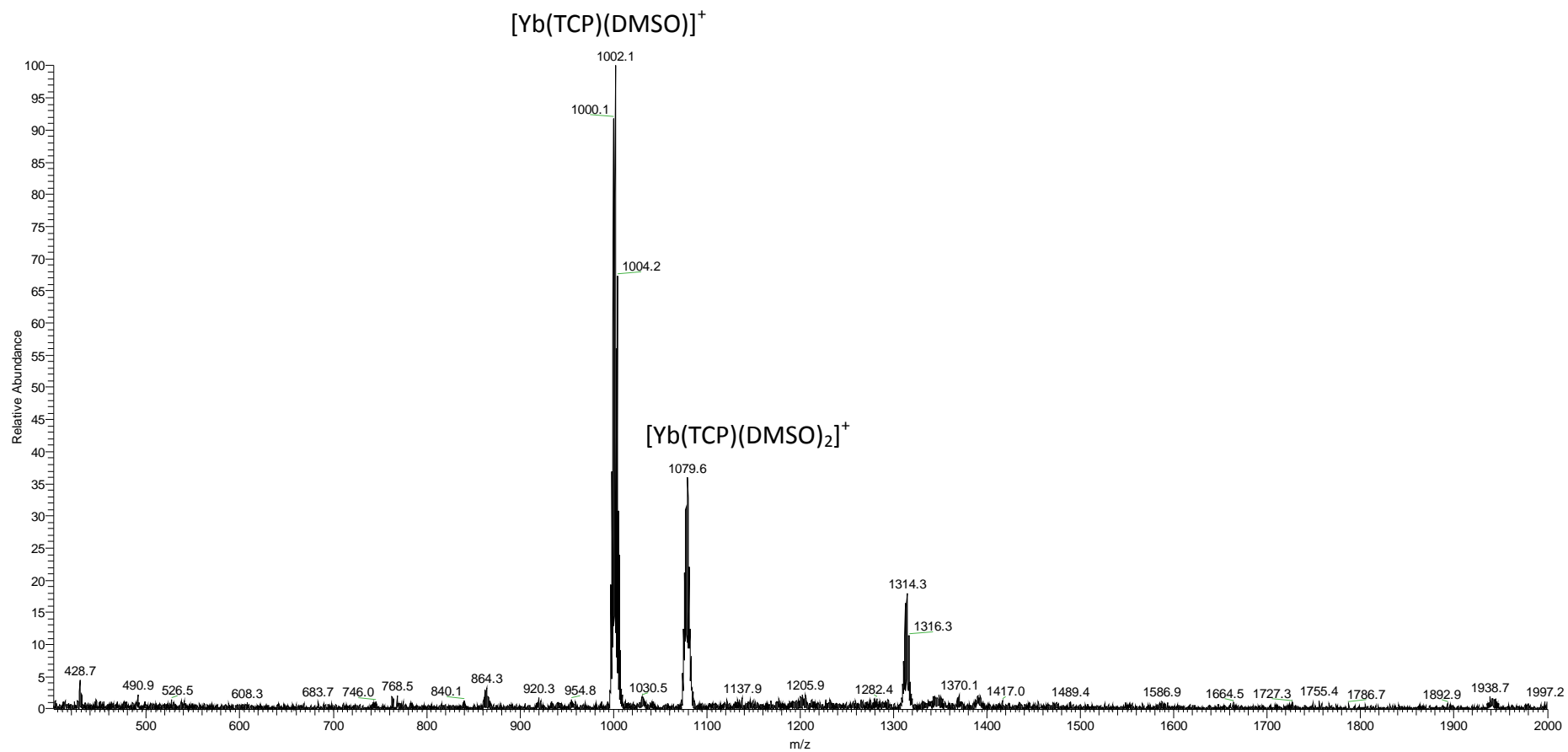


Fig. S6a. Solution stability of **1** in DMSO over 48 h examined by UV-visible spectrophotometry.

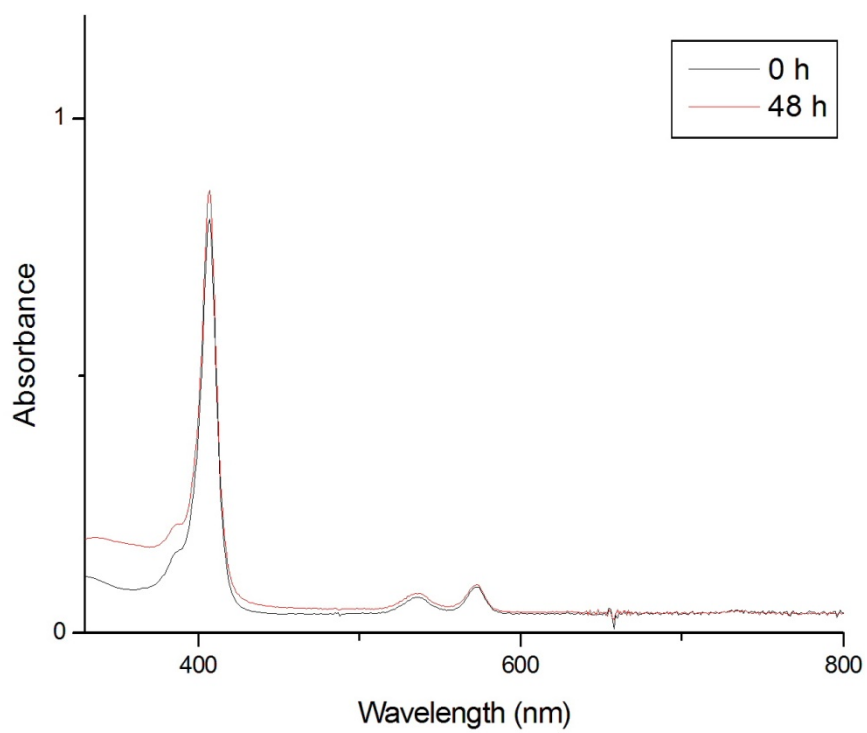


Fig. S6b. Solution stability of **1** in phosphate buffer saline (pH = 7.4) with fetal bovine serum (10%, v/v) over 48 h examined by UV-visible spectrophotometry.

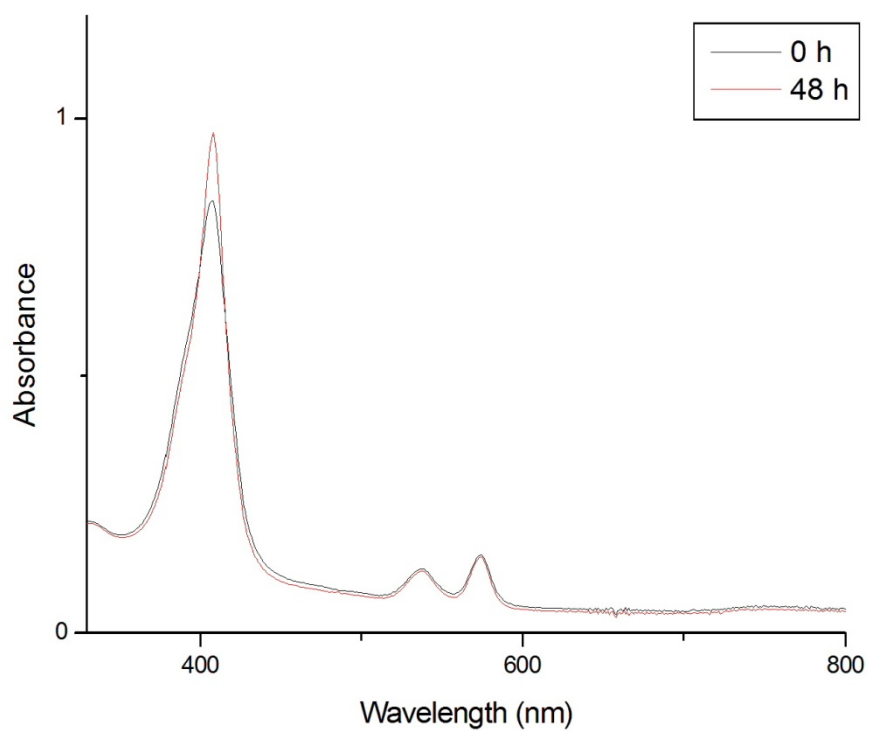


Fig. S6c. Solution stability of **1** in phosphate buffer saline (pH = 7.4) with fetal bovine serum (10%, v/v) and GSH (2 mM) over 48 h examined by UV-visible spectrophotometry.

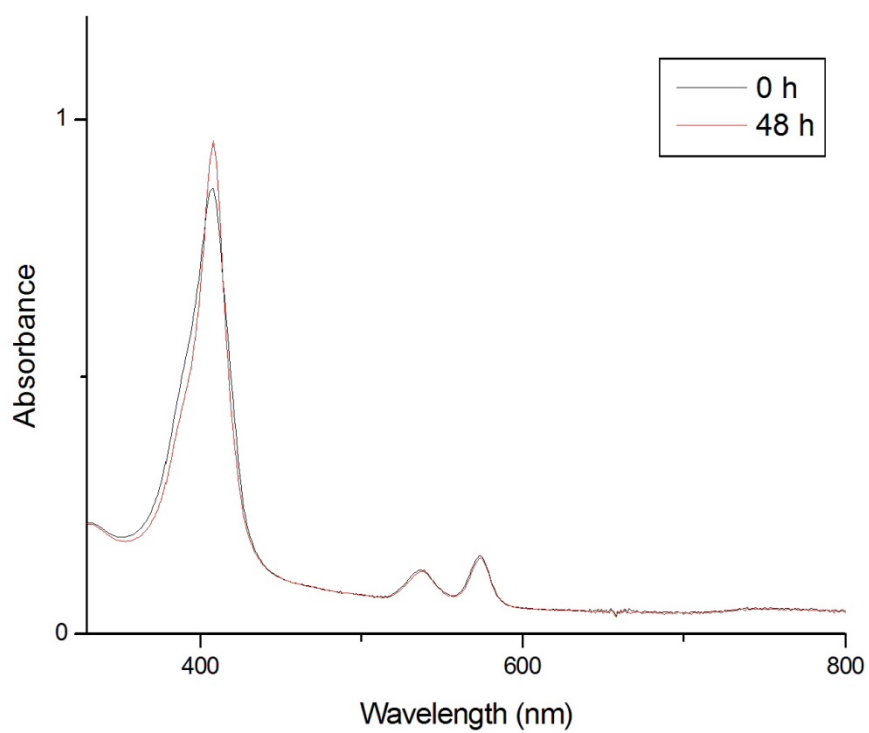


Fig. S6d. Solution stability of **1** in phosphate buffer saline (pH 7.4) with fetal bovine serum (10%, v/v) and sodium citrate (100 μ M) over 48 h examined by UV-visible spectrophotometry.

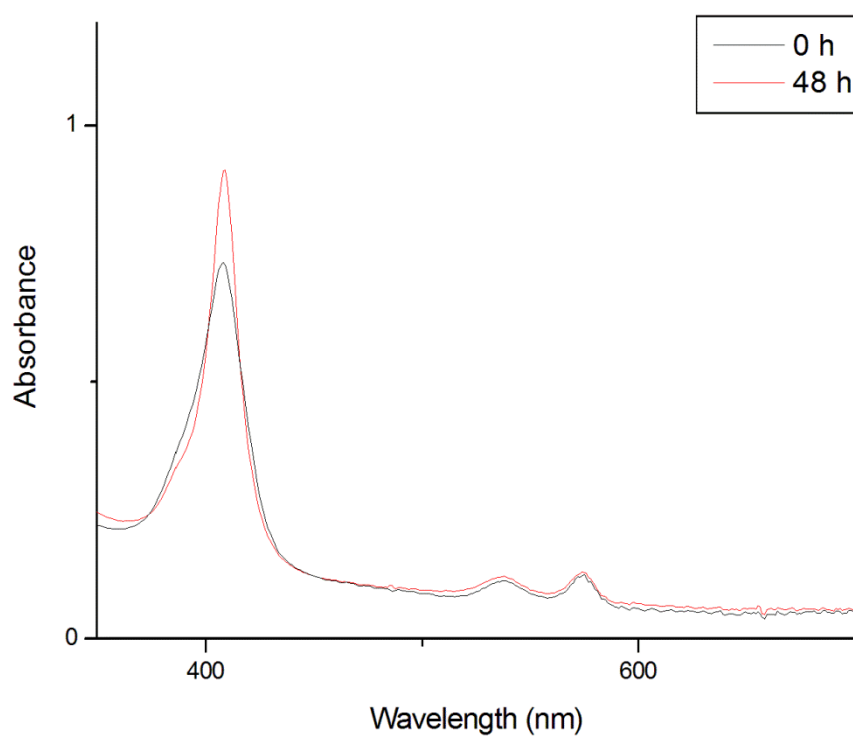


Fig. S7. ESI-MS spectrum of **1** with reduced glutathione (GSH) in DMSO / MeOH / H₂O (1:39:60)

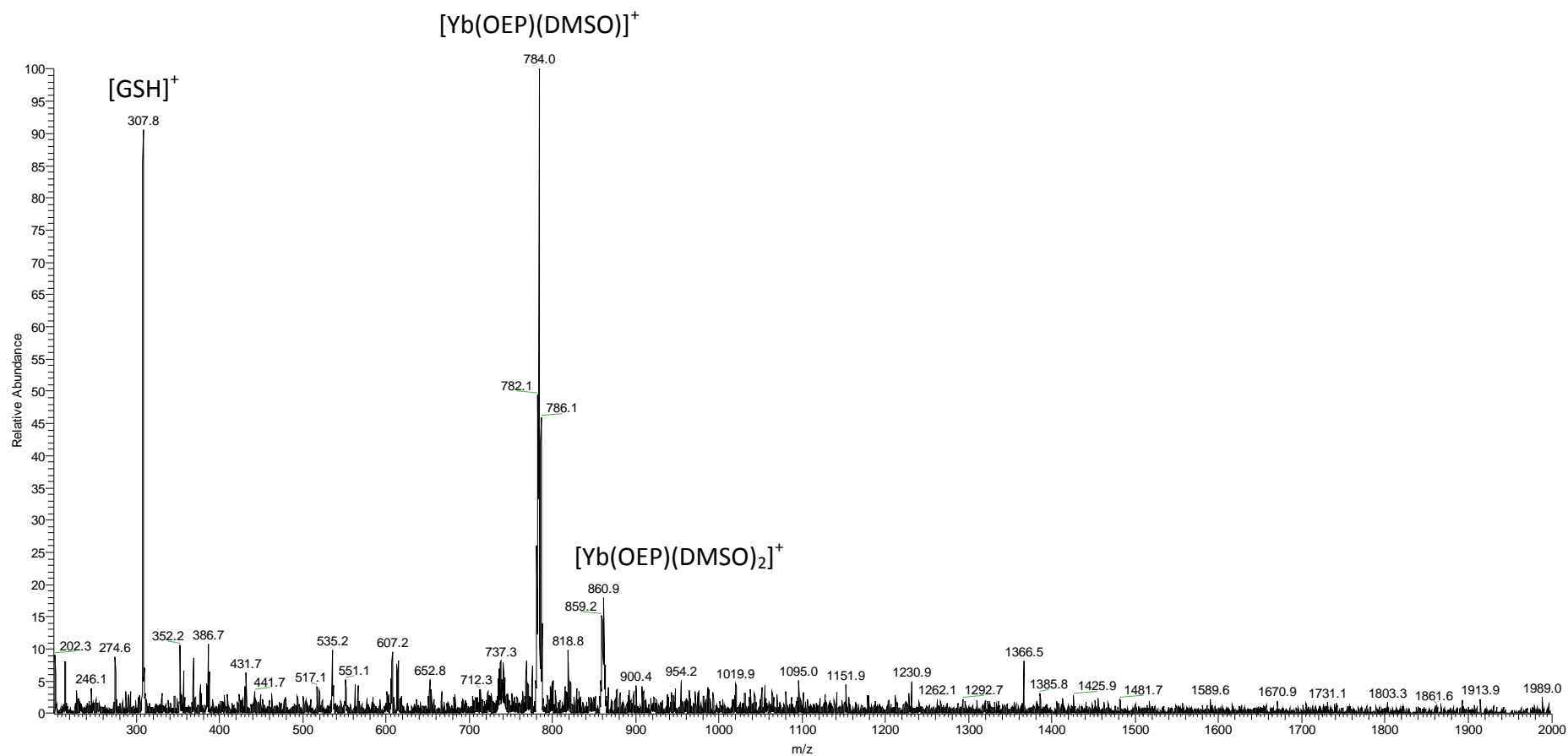


Fig. S8 Complex **1** induces massive cytoplasmic vacuolation in various cancer cell lines. Cells were treated with **1** (1 μ M) for 7 h and the cellular morphologies were examined by light microscopy.

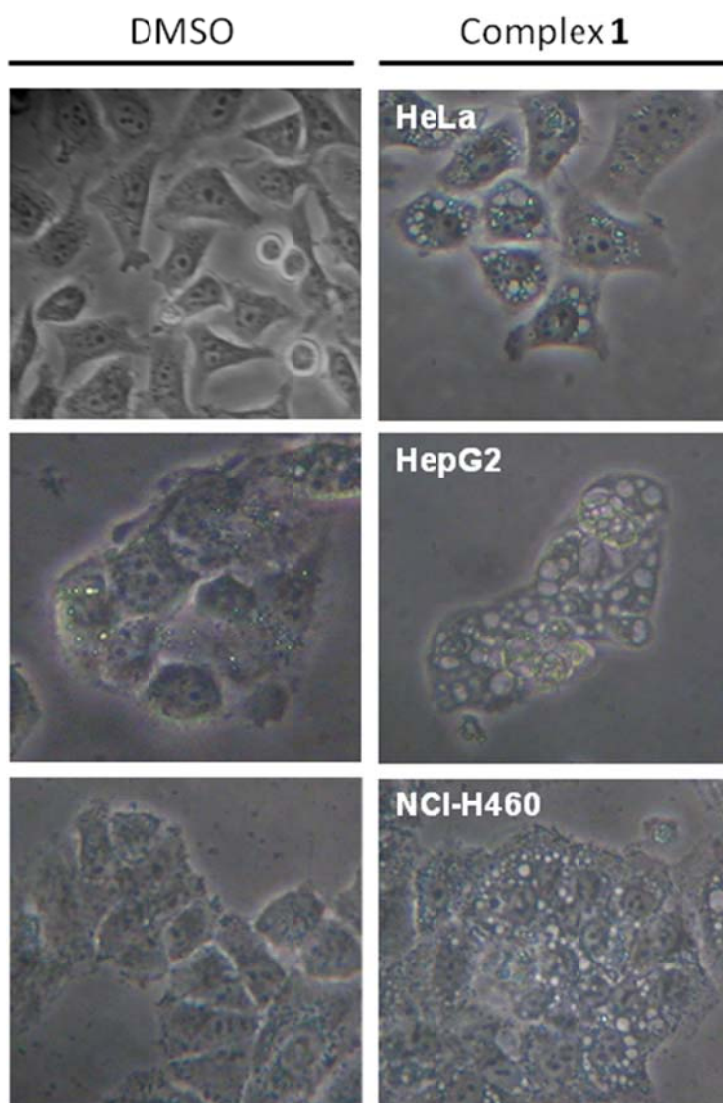


Fig. S9. Dendrogram for clustering experiments, using centered correlation and average linkage. The independent triplicated experiments of **1** are found in the same cluster. This reflects a high reproducibility and reliability of the altered gene expression in HeLa cells by **1**.

